Published in final edited form as:
Oncogene. 2010 December 2; 29(48): 6402–6408. doi:10.1038/onc.2010.360.

c-Src Differentially Regulates the Functions of Microtentacles and Invadopodia

Eric M. Balzer[1,2], **Rebecca A. Whipple**[2], **Keyata Thompson**[2], **Amanda E. Boggs**[1], **Jana Slovic**[1], **Edward H. Cho**[1,2], **Michael A. Matrone**[1,2], **Toshiyuki Yoneda**[3], **Susette C. Mueller**[4], and **Stuart S. Martin**[1,2,5]

[1]Program in Molecular Medicine

[2]Department of Physiology, University of Maryland School of Medicine, Marlene and Stewart Greenebaum NCI Cancer Center, Baltimore MD, 21201

[3]Department of Biochemistry, Osaka University Graduate School of Dentistry, Osaka 565-0871, Japan

[4]Department of Oncology, Lombardi Comprehensive Cancer Center, Georgetown University Medical School, Washington, DC 20057

Abstract

During metastasis, invading cells produce various actin-based membrane protrusions that promote directional migration and proteolysis of extracellular matrix (ECM). Observations of actin staining within thin, tubulin-based *microtentacle* (McTN) protrusions in suspended MDA-MB-231 tumor cells prompted an investigation of whether McTNs are structural or functional analogs of invadopodia. We show here that MDA-MB-231 cells are capable of producing invadopodia and McTNs, both of which contain F-actin. Invadopodium formation was enhanced by expression of a constitutively-active c-Src kinase, and repressed by expression of dominant negative, catalytically-inactive form of c-Src. In contrast, expression of inactive c-Src significantly increased McTN formation. Direct inhibition of c-Src with the SU6656 inhibitor compound also significantly enhanced McTN formation, but suppressed invadopodia, including the appearance of F-actin cores and phospho-cortactin foci, as well as completely blocking focal degradation of extracellular matrix. Additionally, silencing of Tks5 in Src-transformed fibroblasts blocked invadopodia without affecting McTNs. Genetic modification of c-Src activity that promoted McTN formation augmented capillary retention of circulating tumor cells *in vivo* and rapid re-attachment of suspended cells *in vitro*, even though invadopodia were strongly suppressed. These results indicate that McTNs are capable of enhancing tumor cell reattachment, even in the absence of Tks5 and active Src, and define separate cytoskeletal mechanisms and functions for McTNs and invadopodia.

[5]*Corresponding author*, Bressler Building, Rm 10-29, 655 W. Baltimore St., Baltimore, MD 21201, Tel: 410-706-6601, Fax: 410-706-6600, ssmartin@som.umaryland.edu.

Conflict of interest. The authors declare no conflict of interest.

Introduction

Metastatic carcinoma dissemination initiates when epithelial cells in the primary tumor switch to a mesenchymal phenotype that promotes migratory behavior on planar ECM surfaces or within 3-dimensional matrices [1]. This epithelial-to-mesenchymal transition, or *EMT*, increases formation of actin-based plasma membrane protrusions, such as lamellipodia and filopodia, which have precisely defined roles in the locomotion of attached cells along a chemotactic gradient [2, 3]. Migratory cell types also generate protrusions of their ventral surface, such as the podosomes of monocytic and endothelial cells, while carcinoma cells generate invadopodia that localize proteolytic complexes to the ECM-plasma membrane interface, facilitating focal degradation and invasion [4, 5].

Metastasis requires transit through the bloodstream or lymphatic vasculature to reach secondary tissues [6], and therefore necessitates indefinite periods of anchorage-independent survival [7]. Detached tumor cells produce microtubule-rich extensions of the plasma membrane, called microtentacles (McTNs), that promote reattachment of tumor cells to ECM and endothelial monolayers [8–10]. Since extravasation depends on subsequent proteolysis of the endothelial basement membrane, defining the mechanisms that support McTNs and invadopodia will strengthen our understanding of how tumor cells exit the circulation to colonize secondary tissues.

Metastatic breast carcinoma cells were selected to compare and contrast the molecular mechanisms supporting invadopodia and McTNs. We show here that MDA-MB-231 cells produce invadopodia and McTNs, both of which contain a filamentous-actin (F-actin) component. Invadopodia were increased by expression of constitutively-active c-Src protein, but strongly inhibited by dominant-negative c-Src. In contrast, dominant-negative c-Src significantly increased McTN formation, while a similar albeit weaker effect was observed for constitutively active Src. This differential effect of Src on invadopodia and microtentacles was further corroborated by direct inhibition of c-Src with the SU6656 inhibitor compound, which significantly enhanced McTN formation, while suppressing invadopodia. Src-transformation of NIH3T3 fibroblasts induced significant increases in both McTNs and invadopodia, while silencing the invadopodia scaffolding component Tks5 blocked invadopodia, without affecting McTN levels. To assess the biological relevance of these Src-mediated changes in protrusive morphology, *in vivo* lung trapping experiments were performed which demonstrate that McTNs can increase lung retention of circulating tumor cells even in the absence of invadopodia formation. McTNs and invadopodia therefore arise via separate cytoskeletal mechanisms and perform distinct roles during tumor cell reattachment.

Materials and Methods

Cell culture

Bt-549, MDA-MB-231 human mammary carcinoma cells, and all its derivatives were cultured in DMEM (Gibco, CA) containing 10% fetal bovine serum (FBS, Gibco, CA), penicillin/streptomycin (100μg/mL), L-glutamine (2 mmol/L), and 1mg/mL G418 Geneticin (Gibco, CA), and maintained in 5% CO2 at 37°C. c-Src variant cell lines were generated

with chicken c-Src cDNA, and were kind gifts from Dr. Toshiyuki Yoneda. NIH3T3 lines were kind gifts from Dr. Darren Seals. Both the MDA-MB-231 and Bt-549 cell lines have been authenticated as tumorigenic and metastatic *in vivo*.

Microtentacle scoring and live-cell imaging

Adherent cells were incubated with a fluorescent lipophilic dye for 15min. in DMEM (CellMask Orange; 1:2000 Invitrogen, CA), rinsed 3× with PBS and trypsinized. Resuspended cells in duplicate Costar ultra low attachment plates (Corning, NY) were treated with 10μM SU6656, 0.001% DMSO, or no drug, where appropriate. At least 100 single cells in duplicate wells (200/trial) were blindly scored positive for McTNs when displaying motile, flexible plasma membrane protrusions of length equal to or greater than the cell radius. An Olympus CKX41 inverted fluorescent microscope (Melville, NY) equipped with an Olympus F-view II digital camera and Olympus MicroSuite™ Five acquisition software was used for imaging.

McTN immunofluorescence

Approximately 5×10^4 detached cells were fixed in suspension for 10min in 0.5% glutaraldehyde/PBS, and centrifuged at 16×g for 5min onto glass coverslips pre-coated with 1% polyethyleneimine (PEI), permeabilized (0.25% Triton X-100/PBS, 10min), blocked for 1h (10mg/mL BSA/0.5% NP40/PBS), and incubated for 1h at RT with monoclonal anti-α-tubulin (Sigma; 1:1000, DM1A), Phalloidin-Alexa-555 conjugate (Invitrogen; 1:500), or Rabbit polyclonal anti-pY-421 cortactin (Cell Signaling Technologies; 1:500). Secondary detection employed Anti-IgG Alexa Fluor® 488 and 647 (Molecular Probes, CA; 1:1000) and Hoescht 33342 nuclear dye (Sigma; 1:5000) for 1h at room temperature. Images captured on an Olympus IX81 microscope equipped with a Fluoview-1000 confocal laser scanner were analyzed with ImageJ (Bethesda, MD).

Invadopodia imaging and gelatin degradation

12cm round coverslips were inverted on an 80μL drop of fluorescent gelatin solution (0.2% gelatin, (Sigma; 300-bloom) in Dulbecco's modified PBS combined 8:1 with 0.2% gelatin conjugated to Alexa 568) heated to 37°C and placed on parafilm. Coverslips were incubated for 10min, rinsed 3×, fixed in 0.8% glutaraldehyde for 10min, rinsed 3×, and reactive groups quenched (10mg/mL $NaBH_4$, 10min., ice). After 5 rinses, coverslips were placed in the wells of a 24-well plate and seeded with approximately 5×10^4 cells in growth media, then incubated in the presence or absence of 10μM SU6656 (4h, 37°C, 5% CO2). A binary filter was applied to each Fluoview-1000 confocal image to measure area of degraded regions; this was calculated against total-cell area measurements to determine percentage area degraded per cell body. Image analysis was performed in ImageJ (Bethesda, MD).

In vitro attachment assay

An xCelligence RTCA SP real-time cell sensing device (Roche Applied Science, Indianapolis, IN, USA) was used to assess attachment of MDA-231, c-Src527 and c-Src295 lines . Cells (5×10^3) were transferred in quadruplicate into the wells of an E-plate in a

volume of 200μL (Atienza et al., 2006). Cell index is a measure of attachment-induced changes in electrical impedance, and was recorded every 15sec for 1h.

In vivo lung retention assay

MDA-231^{luc} and c-Src295^{luc} cells were detached in enzyme-free cell dissociation buffer and re-suspended at 3×10^6 cells/ml in phosphate-buffered saline. Prior to initial injection and imaging, athymic nude-Foxn1nu mice were injected intraperitoneally with Luciferin (150 mg/kg, Xenogen) and returned to their cages for 5 min. A 100uL volume containing 3×10^5 cells was then injected intravenously into the tail vein of animals restrained by mouse tail illuminator, tail vein injection apparatus (Braintree Scientific, Braintree, MA, USA). Mice were anesthetized with 2% isoflurane gas and imaged for 5min under single-photon emission. Total photon flux (photons/sec) was calculated and corrected for tissue depth and background signal via spectral imaging in Living Image 3.0 software (Xenogen). Subsequent images were used to calculate percent signal (photon flux) at a series of time points relative to initial values.

Results and Discussion

The ability of circulating tumor cells to escape the bloodstream is a key determinant of metastatic efficiency [11], but the specific cytoskeletal mechanisms by which tumor cells successfully extravasate into distant tissues remain unclear. Given the rapid transitions in tumor cell attachment during metastasis, it is likely that the cytoskeletal dynamics of both detached and adherent tumor cells contribute to extravasation. While adherent tumor cells form pseudopodia and invadopodia that penetrate endothelial cell junctions and remodel underlying ECM [12, 13], our previous work has implicated a preceding role for McTNs during the initial engagement of detached tumor cells to the endothelium [9, 10]. We examined the cytoskeletal mechanisms underlying invadopodia and McTNs using MDA-MB-231 metastatic human breast carcinoma cells. When allowed to attach to gelatin for 4h, MDA-MB-231 cells formed invadopodia with characteristic F-actin cores that co-aligned with degraded areas of the gelatin (figure 1A, top row). No similar concentrations of α-tubulin could be seen within these foci (data not shown), consistent with previous reports that actin is the primary cytoskeletal component of invadopodia [14]. To determine the structural makeup of McTNs in MDA-MB-231s, cells fixed in suspension were labeled for F-actin and α-tubulin (figure 1A, bottom row), showing that these cells form numerous protrusions that co-stain for α-tubulin and F-actin. Detached MDA-MB-231 cells therefore produce McTNs with an F-actin component that are structurally distinguished from invadopodia by the presence of microtubules. The same results were also observed in Bt-549 cells (figures S1 and S2).

The proto-oncogenic tyrosine kinase c-Src is both necessary and sufficient for the formation of invadopodia at sites of integrin-mediated ECM adhesion [15]. To examine the role of Src in McTN formation, we used MDA-MB-231 cells stably expressing constitutively-active (c-Src527), and dominant-negative (c-Src295) c-Src variants. Significant variations in McTN production were observed for these cells (figure 1B). Both mutant lines exhibited increases in McTN frequency relative to the parental line, with an increase of 149% in the dominant-

negative c-Src295 expressing cells, relative to the parental control. In contrast, c-Src295 repressed the formation of invadopodia, while c-Src527 promoted invadopodia (figure 1C) that were identified by characteristic F-actin cores co-localized with phosphorylated-cortactin puncta, and digested spots in the fluorescent gelatin matrix [16]. The inverse effects that dominant-negative Src has on McTNs and invadopodia indicates that separate mechanisms control these two structures. In addition, the lack of degradative capacity in the high-McTN c-Src295 line indicates that McTNs are not directly involved in proteolytic ECM degradation, suggesting that McTNs and invadopodia provide separate functions for the metastatic tumor cell.

To exclude the possibility that long-term adaptations of the c-Src295 and c-Src527 cell lines produced the varied McTN and invadopodia phenotypes, we transiently inhibited c-Src activity with the cell-permeable SU6656 inhibitor compound, which was chosen on the basis of its high affinity and selectivity for Src family kinases, relative to the PP1 and PP2 Src inhibitors, which are also potent inhibitors of PDGFR activity [17]. Treatment of c-Src527 cells with 10μM SU6656 for 1h suppressed the activity of c-Src, as measured by immunodetection of tyrosine-416 autophosphorylation (figure 2A). As expected, the c-Src activity remained low in c-Src295 cells. Incubation with SU6656 reduced invadopodia formation (figure 2B), leading to reductions in ECM degradation that were strongest (21-fold) in the c-Src527 cells, which have high basal levels of invadopodia (figure S3).

Having observed the suppression of invadopodia by c-Src inhibition, we proceeded to examine the effects of SU6656 on suspended MDA-MB-231 cells and both c-Src variants. Acute c-Src inhibition induced a marked increase in McTN frequency, and morphological changes characterized by dramatically augmented McTN length (figure 2C). Blinded quantitative scoring demonstrated that c-Src inhibition with SU6656 significantly increased McTNs in all three cell lines (figure 2D). This increase was nearly 4-fold above vehicle control conditions for the parental MDA-MB-231, and 2-fold for c-Src527 cells. The integrity of the cortical actin cytoskeleton is an important regulator of McTN formation[8–10], therefore increases in Src kinase activity may indirectly promote increases in McTNs formation by stimulating cytoskeletal rearrangement.(Figure 2A). Interestingly, this response occurred to an even greater extent when c-Src activity was suppressed, indicating that a lack of src signaling also results in cytoskeletal modifications that promote McTN formation. Since integrin engagement is necessary for c-Src activation [18], the changes in tumor cell attachment during metastasis produce different Src activation states, as confirmed by western blotting of ECM-bound and detached cell populations (figure S4).

To further examine the involvement of invadopodia in Src-induced McTN changes, invadopodia were targeted independently of c-Src function by shRNA-mediated silencing of the scaffold/adaptor protein Tks5/Fish, which is required for invadopodia function[19]. Src-transformed 3T3 fibroblasts expressing reduced levels of Tks5 (figure 3A, clones 4.20 and 4.24)), formed fewer invadopodia than their non-silencing control (clones C1 and C2), and parental counterparts (Src3T3) (figure 3B). Src-transformed 3T3 cells exhibited McTN increases of 265% over parental controls, consistent with similar increases in c-Src 527 MDA-231 cells, and c-Src inhibition in these cells further enhanced McTN frequency to nearly all cells in a given population. Importantly, no relationship could be established

between invadopodia function and McTN formation, demonstrating that these two forms of cellular protrusion are mechanistically distinct. (figure 3C).

Accumulating evidence supports two broad phases through which disseminated tumor cells extravasate from systemic circulation. We propose that the early stage of this process occurs when circulating cells arrest in the vasculature and contact the endothelium. Intravital imaging studies show that initial adhesion of circulating tumor cells to capillary walls is tubulin-dependent, and actually enhanced by depolymerization of F-actin [20]. Recent work also demonstrates that microtubule stabilization can actually promote adhesion of suspended tumor cells to ECM [10]. Since McTNs are enriched in microtubules, and are enhanced by actin depolymerization [8, 9], these findings implicate a role for McTNs in endothelial docking during early extravasation. To determine the effects of c-Src modification on endothelial adhesion, dominant negative c-Src295 and parental MDA-231 cells expressing luciferase were injected into the tail vein of mice, and imaged over a 6 hour time-course. The injected population was detectable in the lungs by 15 minutes post-injection, and was monitored over a 48h period to allow cells to be pushed beyond the pulmonary capillary beds. The proportion of cells retained in the lungs was measured by total photon flux at select times and normalized to initial values. Figure 4 shows that suppression of c-Src activity significantly enhanced trapping and retention of CTCs in lung capillaries relative to MDA-231 parental cells. This trend was observable by 2 hours, and showed significant separation over the next 46 hours. Additionally, both positive and negative modification of c-Src activity enhanced early rates of attachment to an extracellular substrate *in vitro* (figure S5). These data indicate that McTN-inducing modifications of c-Src activity promote tethering and persistence of disseminated tumor cells in secondary sites, even when invadopodia are suppressed.

Trans-endothelial migration, being the second proposed phase in this model of extravasation, follows transient substrate tethering and requires a separate set of cytoplasmic functions that are dependent on permanent ECM-contact. Examples of the latter include focal adhesions and invadopodia, which are coordinated by the cell to provide the traction, tensile F-actin forces, and proteolysis of the basement membrane necessary for invasion into the surrounding stroma[5]. Invadopodia and many other aspects of migratory cell behavior are directly regulated by c-Src, and we find that c-Src can also affect McTN formation. In light of the fact that both Src-transformed and c-Src deficient cells produce more McTNs than their wildtype parents, this appears to represent an indirect regulation that results from overall alterations in cytoskeletal architecture, rather than specifically defined substrate interactions. These data support a model in which the detachment of tumor cells modifies c-Src activity in a manner that induces cortical F-actin rearrangements which are permissive for McTN formation, ultimately promoting adhesion to other hematogenous cell types or capillary endothelium. Once permanent ECM-contacts are formed, signaling through c-Src then renews adherent cytoskeletal conformations that suppress McTNs, and coordinates Tks5 and cortactin to promote invadopodia and tumor cell invasion. From a clinical perspective, these results emphasize the importance of considering the unintentional effects of cytoskeletally-targeted drugs on detached and circulating tumor cells. While inhibiting Src activity could temporarily reduce the invasive behavior of adherent cells, the resulting

increase in McTNs may actually enhance the reattachment and survival of circulating tumor cells in secondary sites and elevate metastatic risk.

Supplementary Material

Refer to Web version on PubMed Central for supplementary material.

Acknowledgments

Grant support: R01-CA124704 from National Cancer Institute and Breast Cancer Idea Award from USA Medical Research and Materiel Command (BC061047). We are very grateful to Darren Seals and Sara Courtneidge for generously providing cell lines and reagents to examine the role of Tks5.

Abbreviations

ECM	extracellular matrix
McTN	microtentacle
F-actin	filamentous actin
PDGFR	platelet derived growth factor receptor

References

1. Yilmaz M, Christofori G. EMT, the cytoskeleton, and cancer cell invasion. Cancer Metastasis Rev. 2009; 28(1–2):15–33. [PubMed: 19169796]
2. Gupton SL, Gertler FB. Filopodia: the fingers that do the walking. Sci STKE. 2007; 2007(400):re5. [PubMed: 17712139]
3. Machesky LM. Lamellipodia and filopodia in metastasis and invasion. FEBS Lett. 2008; 582(14): 2102–2111. [PubMed: 18396168]
4. Linder S. The matrix corroded: podosomes and invadopodia in extracellular matrix degradation. Trends Cell Biol. 2007; 17(3):107–117. [PubMed: 17275303]
5. Buccione R, Caldieri G, Ayala I. Invadopodia: specialized tumor cell structures for the focal degradation of the extracellular matrix. Cancer Metastasis Rev. 2009; 28(1–2):137–149. [PubMed: 19153671]
6. Mendoza M, Khanna C. Revisiting the seed and soil in cancer metastasis. Int J Biochem Cell Biol. 2009; 41(7):1452–1462. [PubMed: 19401145]
7. Mehlen P, Puisieux A. Metastasis: a question of life or death. Nat Rev Cancer. 2006; 6(6):449–458. [PubMed: 16723991]
8. Whipple RA, Cheung AM, Martin SS. Detyrosinated microtubule protrusions in suspended mammary epithelial cells promote reattachment. Exp Cell Res. 2007; 313(7):1326–1336. [PubMed: 17359970]
9. Whipple RA, et al. Vimentin filaments support extension of tubulin-based microtentacles in detached breast tumor cells. Cancer Res. 2008; 68(14):5678–5688. [PubMed: 18632620]
10. Balzer EM, et al. Antimitotic chemotherapeutics promote adhesive responses in detached and circulating tumor cells. Breast Cancer Res Treat. 2010; 121(1):65–78. [PubMed: 19593636]
11. Chambers AF, Groom AC, MacDonald IC. Dissemination and growth of cancer cells in metastatic sites. Nat Rev Cancer. 2002; 2(8):563–572. [PubMed: 12154349]
12. Miles FL, et al. Stepping out of the flow: capillary extravasation in cancer metastasis. Clin Exp Metastasis. 2008; 25(4):305–324. [PubMed: 17906932]
13. Clark ES, Weaver AM. A new role for cortactin in invadopodia: regulation of protease secretion. Eur J Cell Biol. 2008; 87(8–9):581–590. [PubMed: 18342393]

14. Buccione R, Orth JD, McNiven MA. Foot and mouth: podosomes, invadopodia and circular dorsal ruffles. Nat Rev Mol Cell Biol. 2004; 5(8):647–657. [PubMed: 15366708]

15. Frame MC, et al. v-Src's hold over actin and cell adhesions. Nat Rev Mol Cell Biol. 2002; 3(4): 233–245. [PubMed: 11994743]

16. Linder S, Aepfelbacher M. Podosomes: adhesion hot-spots of invasive cells. Trends Cell Biol. 2003; 13(7):376–385. [PubMed: 12837608]

17. Blake RA, et al. SU6656, a selective src family kinase inhibitor, used to probe growth factor signaling. Mol Cell Biol. 2000; 20(23):9018–9027. [PubMed: 11074000]

18. Mitra SK, Schlaepfer DD. Integrin-regulated FAK-Src signaling in normal and cancer cells. Curr Opin Cell Biol. 2006; 18(5):516–523. [PubMed: 16919435]

19. Seals DF, et al. The adaptor protein Tks5/Fish is required for podosome formation and function, and for the protease-driven invasion of cancer cells. Cancer Cell. 2005; 7(2):155–165. [PubMed: 15710328]

20. Korb T, et al. Integrity of actin fibers and microtubules influences metastatic tumor cell adhesion. Exp Cell Res. 2004; 299(1):236–247. [PubMed: 15302590]

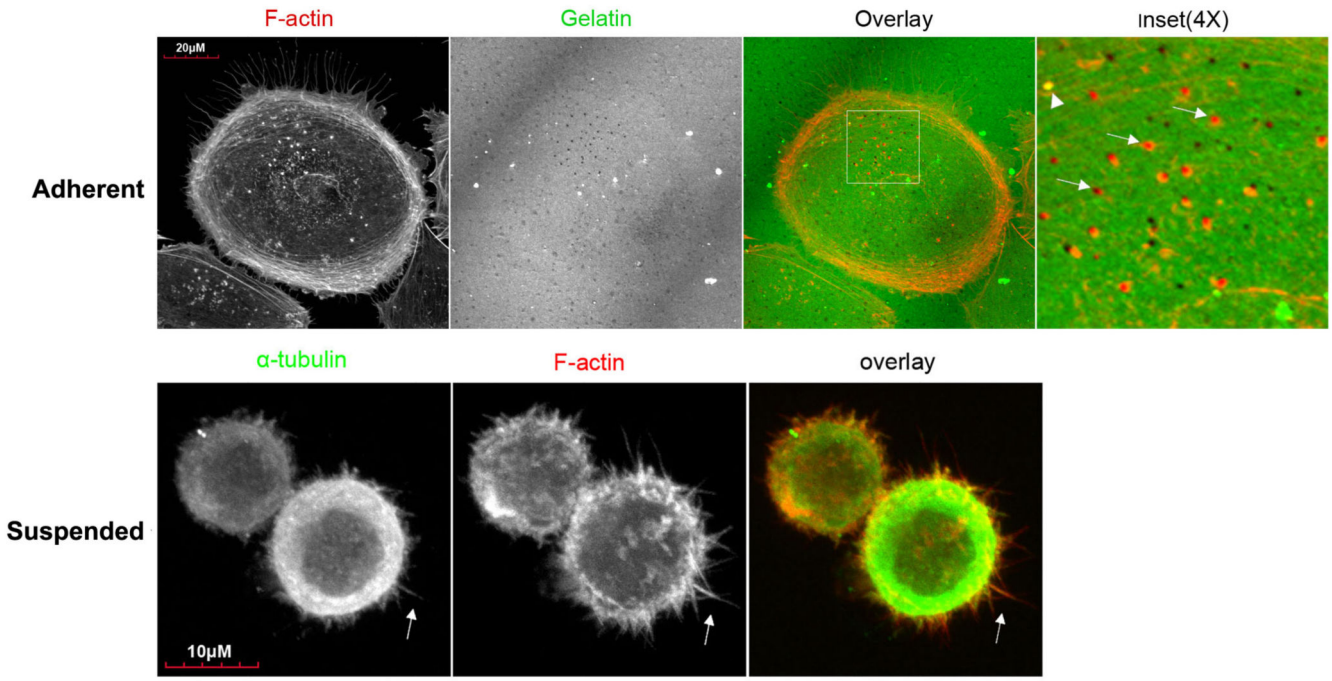

Figure 1. MDA-MB-231s form invadopodia and microtentacles, in a manner that is affected by c-Src activation

(A) Top row: When cultured for 4h on a thin layer of fluorescently-conjugated gelatin, MDA-MB-231 cells form focal areas of digested matrix that appear as dark spots or 'holes' (second panel) co-localizing with bright F-actin cores (Inset panel magnifies boxed region of overlay panel; arrowhead indicates an undigested region, while arrows point to degraded holes). Bottom row: Fixation of suspended cells revealed extensive plasma membrane protrusions (arrows) that co-stained for α-tubulin (left panel) and F-actin (middle panel). (B) McTN incidence is greatest in cells with dominant-negative c-Src295 (* denotes significant change relative to parental control, $p<0.0001$, $n=12$). (C) Immunofluorescence reveals that dominant-negative c-Src295 suppresses invadopodia formation and focal gelatin degradation, despite enhancing McTNs (suspended panel). Inset panels show 2X magnification of boxed region.

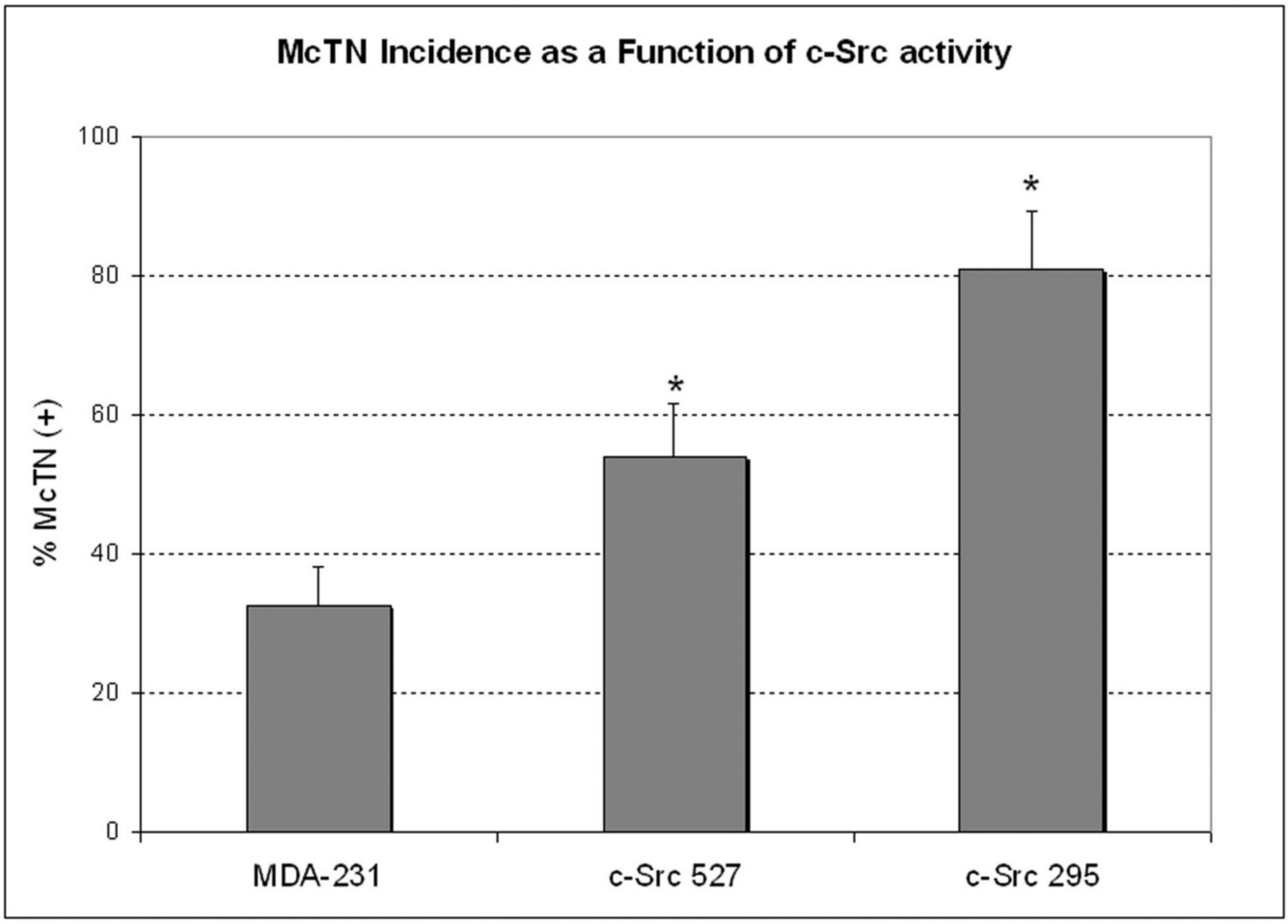

Figure 2. Acute c-Src inhibition inversely affects invadopodia and microtentacles

(A) Treatment of c-Src527 cells with SU6656 (10μM, 1h) suppressed phosphorylation of the activating tyrosine-416 residue, while c-Src295 cells showed only minimal kinase activation. (B) Exposure to 10μM SU6656 completely blocked invadopodia formation in c-Src-527 cells, as identified by co-labeling of phosphorylated cortactin puncta with F-actin cores, and gelatin holes. These features are clearly visible under vehicle control conditions (top row), but are lost when c-Src is inhibited (bottom row) Inset panels show 2X magnification of boxed region. (C) 10μM SU6656 enhanced the formation of McTNs in all cell lines examined. Arrows indicate long McTN extensions that resulted from c-Src inhibition (parental 231s, and c-Src-527s); comparably long extensions were observed basally in c-Src-295s (arrowheads), though at a lower frequency. (D) Blinded quantification revealed that McTN formation was significantly enhanced by SU6656, even in cells with low amounts of residual c-Src activity (* denotes significant changes relative to vehicle control, $p<0.0001$).

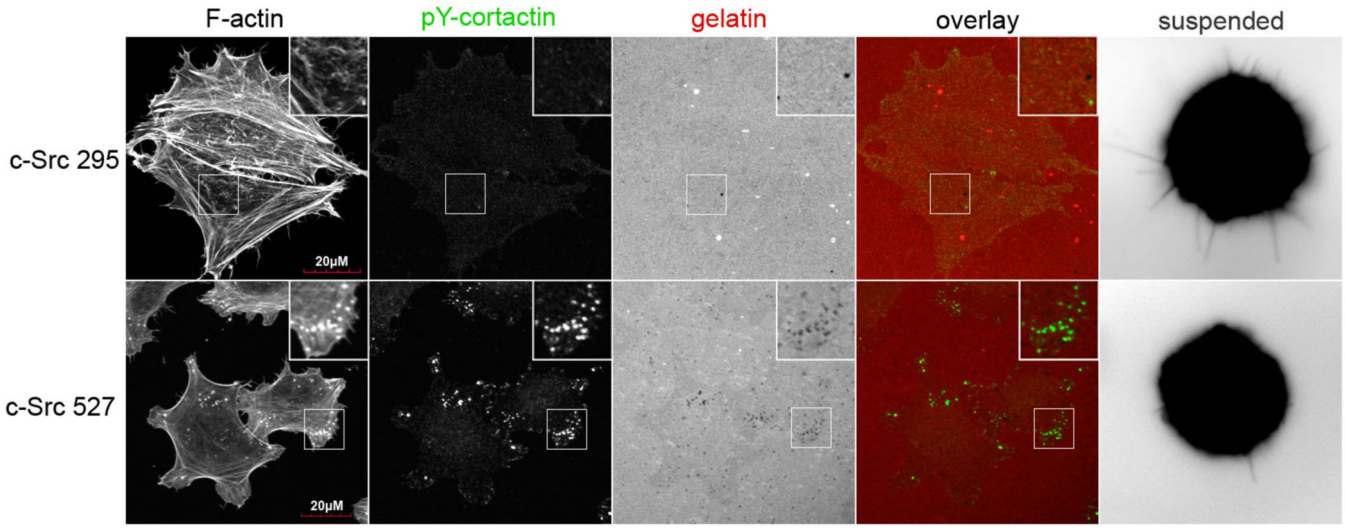

Figure 3. Tks5 silencing blocks invadopodia but does not affect McTN formation

(A) Src transformed NIH 3T3 cells (lane 2) were tested relative to clones that express non-silencing control shRNAs (C1 and C2: lanes 3 and 4), and shRNAs complementary to Tks5/Fish (4.20, and 4.24: lanes 5 and 6). These clones were lysed and total protein fractions were probed for Tks5/Fish via SDS-PAGE to demonstrate efficient Tks5 knockdown. Parental 3T3 cells are represented in lane 1, and an actin loading control is shown in the bottom row. (B) Gelatin degradation of Src 3T3 Tks5 clones was assayed by immunofluorescence. Src 3T3 and Src 3T3 C1 cells efficiently and rapidly formed invadopodia by 2 hours that co-localized with Tks5/Fish (inset panels, top and middle rows), while the Tks5 knockdown clone 4.24 showed a significant reduction in invadopodia formation and focal degradation, in agreement with previous reports [19]. (C) Microtentacle scoring over multiple independent trials (n=9) revealed an increase in McTNs among Src-transformed clones that was further enhanced by acute Src inhibition (t=30 minutes).

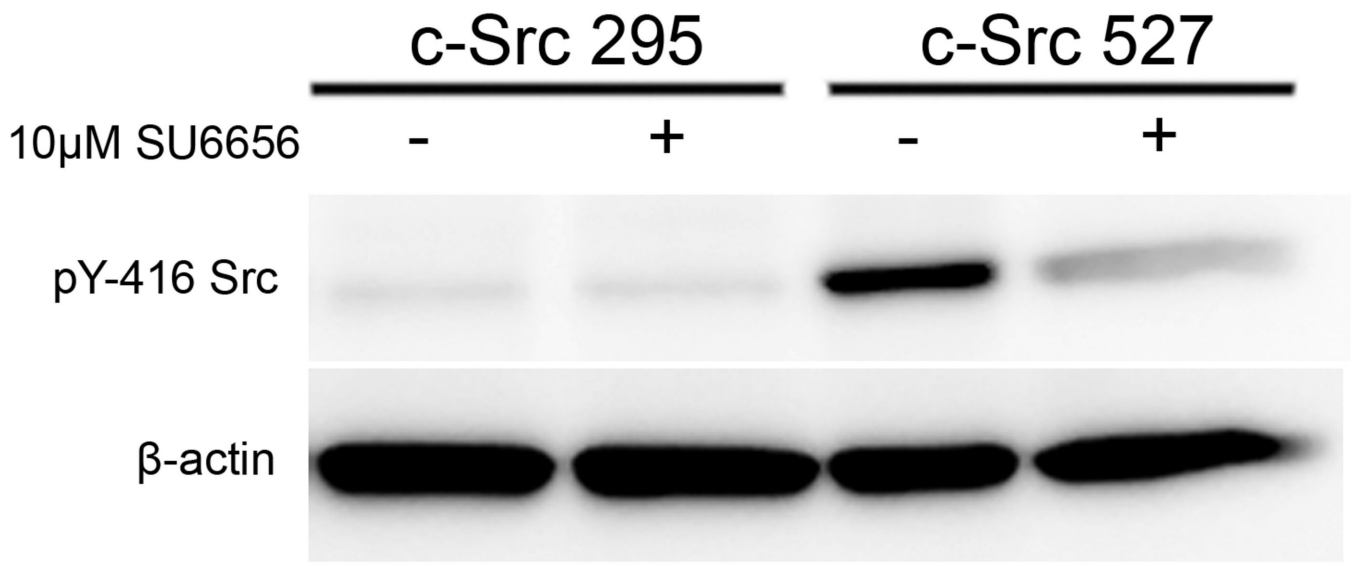

Figure 4. Capillary retention of circulating tumor cells is enhanced by alterations in c-Src activity

(A) Luciferase-expressing cells were injected into the tail vein of live mice and imaged in the presence of luciferin at selected timepoints, over a period of 2 days. c-Src295 cells were trapped and retained more efficiently in the lung capillaries throughout this time course, relative to MDA-231 parental cells. Reported are the average values of c-Src295 (n=14) and MDA-231 (n=10) over three independent trials. Asterisks denote significant differences in signal retention between cell lines (*: $p<0.01$, **: $p=0.05$). (B) Representative images were selected to demonstrate the retention over time of tumor cells in the lungs of a single mouse injected with either MDA-231 parental cells, or C-Src 295 cells. Temperature scale bar indicate absolute values for photon flux at each timepoint.